
Article:
Mendes, AC, Strohmenger, T, Goycoolea, F orcid.org/0000-0001-7949-5429 et al. (1 more author) (2017) Electrostatic self-assembly of polysaccharides into nanofibers. Colloids and Surfaces A: Physicochemical and Engineering Aspects, 531. pp. 182-188. ISSN 0927-7757

https://doi.org/10.1016/j.colsurfa.2017.07.044

Electrostatic self-assembly of polysaccharides into nanofibers

Ana C.Mendes[a*] Timm Strohmenger[b] Francisco Goycoolea[b,c] Ioannis S.Chronakis[a]

[a]Nano-BioScience Research Group, DTU-Food, Technical University of Denmark, Kemitorvet 202, 2800 Kgs. Lyngby, Denmark

[b] Institute for Biology and Biotechnology of Plants (IBBP), Westfälische Wilhelms-Universität Münster, Schlossgarten 3, 48149 Münster, Germany

[c] School of Food Science and Nutrition, University of Leeds, Leeds LS2 9JT, United Kingdom

Abstract

In this study, the anionic polysaccharide Xanthan gum (X) was mixed with positively charged Chitosan oligomers (ChO), and used as building blocks, to generate novel nanofibers by electrostatic self-assembly in aqueous conditions. Different concentrations, ionic strength and order of mixing of both components were tested and observed to affect the diameter, which ranged from 100 to 500 nm, and morphology of the self-assembled nanofibers. The release of diclofenac, as model drug, from self-assembled xanthan-chitosan nanofibers was demonstrated, suggesting that these nanostructures can be used in applications within life sciences such as drug delivery.

Graphical abstract

*Corresponding Author

anac@food.dtu.dk

1. Introduction

Self-assembly, the ubiquitous process used by nature to create complex nanostructures with outstanding functionalities [1], has been explored for developing bio-inspired materials with enhanced properties such as flexibility, hierarchical order and bioactivity [1–5]. Different material geometries have been produced by self-assembly, including fibers. Due to their high surface area, tunable diameter and surface functionality, the use of fibers have been explored in numerous applications, including food, drug delivery and tissue engineering. The phenomenon of polyelectrolyte complexation to form self-assembled fibers using only polysaccharides as building blocks was reported initially by Yamamoto [6], where it was found that interactions of the oppositely charged polyelectrolytes (chitosan and gellan gum) at the interface in aqueous solutions gave rise to regular droplet, honeycomb, sphere and fiber structures. Later a similar approach was developed, where chitosan and alginate where combined to form self-assembled fibers via polyelectrolyte complexation to encapsulate proteins and cells [7]. For the fabrication of self-assembled fibers, a minimum concentration of polyelectrolyte is needed for continuous fiber drawing. In addition, higher molecular weight polyelectrolytes draw better the formation of fibers due to their ability to form a more viscous complex that stabilizes the interface. Their larger area and segments can support interaction and facilitate complexation [19]. Though, the investigation and development of other fiber systems using other relevant polysaccharides by self-assembly is still scarce.

Xanthan gum (X), an anionic extracellular polysaccharide produced by the bacterium Xanthomonas campestris[8–10] has been used as building block to generate self-assembled structures [3–5] with potential use in tissue engineering, regenerative medicine, controlled drug delivery. Xanthan's primary structure consists of α(1 → 4)-linked glucose units substituted at O-3 of alternate glucose residues, with a trisaccharide composed of one glucuronic acid unit between two mannose units containing acetyl group and pyruvate residues (Fig. 1a).

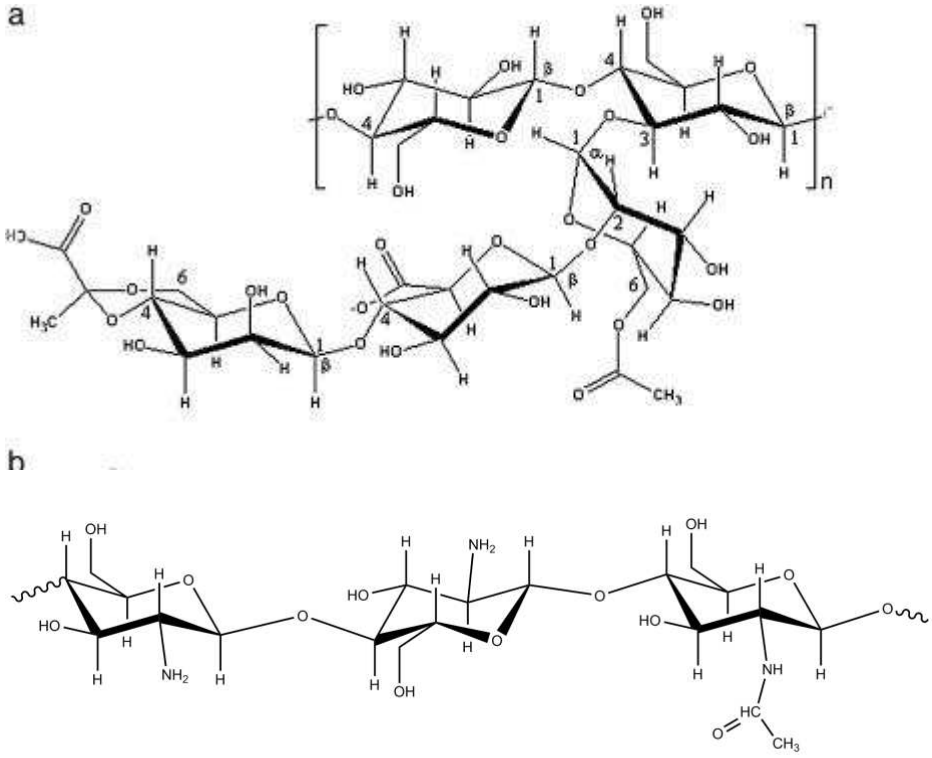

Fig. 1. Chemical structure of (a) xanthan repeating unit and (b) a representative structure of a chitosan, showing residues of β(1.4)-linked 2-amino-2-deoxy-D-glucose (D residues) and N-acetyl-2-amino-2-deoxy-D-glucose (A residues).

Chitosan's are positively charged polysaccharides, consisting of glucosamine linked to N-acetyl glucosamine units, that can exhibit several biological properties such as biocompatibility, biodegradability, hemostatic activity, antibacterial, antimycotic and anticoagulant activity [11–14]. Chitosan oligomers (ChO) are a class of water-soluble chitosan(s) with relatively low molecular weight obtained by the depolymerization of Chitosan(s), comprising also a set of bioactive properties [15] (Fig. 1b). Chitosan oligomers have been used as anti-microbial agents and also as absorption enhancers to improve pulmonary absorption of interferon-α in rats, intestinal absorption of insulin and FD4 and oral absorption of low molecular weight heparin [16]. Xanthan-chitosan complexes using non-oligomeric chitosan's have been prepared as microcapsules [17], gel tablets [13], hydrogels [18], macroporous structures and beads [13] for drug delivery applications.

However, the combination of xanthan gum with positively charged low molecular weight chitosan's, such as ChO to generate self-assembled polyelectrolyte

nanostructures with tuned morphologies, such as nanofibers has never been reported. Therefore, in this work, the anionic polysaccharide xanthan gum was mixed with the positively charged low Mw chitosan to generate nanofibers by electrostatic self-assembly in aqueous conditions. Different concentrations, ionic strength and order of mixing of chitosan oligomers and xanthan were tested and the effect of these parameters was investigated in terms of the morphology of the self-assembled nanofibers. Furthermore, diclofenac, a water soluble Non-Steroidal Anti-inflammatory Drug (NSAID), known for its potent anti-inflammatory, analgesic and antipyretic properties [20], was used as model drug, to test the potential of self-assembled X-Ch nanofibers as drug delivery carrier.

2. Experimental

2.1. Materials

Xanthan gum (Mw 990 kDa [21]), with reference Cosphaderm® X 34, was obtained from Cosphatec, Germany. Chitosan Oligomers (Mw < 5 Da) was obtained from Heppe Medical Chitosan GmbH, Germany. All chemicals were obtained from Sigma/Aldrich (USA) unless otherwise indicated and used as received.

2.2. Sample preparation

Xanthan gum (X) was dissolved in distilled water and NaCl 15 mM at the concentration of 0.6 mg/mL. Chitosan oligomers (ChO) were dissolved in distilled water and NaCl 15 mM at the concentrations of 0.1, 0.6 and 1 mg/mL. Both solutions were allowed to stir overnight at room temperature. The development of the nanostructures took place on a 96-well plate by adding ChO solution on top of xanthan solution or by adding xanthan solution on top of ChO solution.

2.3. Polarimetry

Measurements of variation of optical rotation of xanthan gum were conducted in a JASCO P-2000 polarimeter at 436 nm, using temperatures of 15, 25 and 37 ℃. Xanthan gum samples were dissolved at concentration of 0.6 mg/mL in H_2O and various salt gradients of NaCl ranging from 0 to 100 mM.

2.4. Zeta potential (ζ)

Zeta potential (ζ) was measured at 25 ℃ on a Zetasizer (Nano-ZS ZEN 3600, Mal vern Instruments, UK) to investigate the charge of the X and ChO oligomers at different ionic strength and concentrations. Samples were equilibrated for 2 min at the desired temperature before measurements.

2.5. Turbidity studies

Turbidity measurements were performed after mixing X with ChO to provide information about interactions between both components and compared with the individual components as controls. Turbidity experiments were conducted in a PowerWave™ HT Microplate Spectrophotometer (BioTek Instruments, UK). Turbidity profile of X, ChO and X-ChO solutions were assessed by the change in absorbance at wavelength of 630 nm after 10 and 60 min. These studies were conducted in triplicate for each condition [n= 3].

2.6. Scanning electron microscopy (SEM)

SEM imaging was used to examine the nanoarchitecture of the self-assembled X-ChO nanofibers. The structures were fixed in 2.5% (v/v) glutaraldehyde (in phosphate buffer solution (PBS), pH 7.4) for 1 h. The samples were then dehydrated in a graded ethanol series (50, 70, 90, 96 and 100%) followed by immersion in hexamethyldisilazane (HMDS) [2]. For SEM, the specimens were mounted on aluminum stubs and sputter-coated with gold prior to the visualization on a scanning electron microscope Quanta FEG 3D SEM. The diameters of the electrospun fibers were measured using an image visualization software Image-J (National Institutes of Health, USA). Data Analysis: Student's T-test was applied to determine statistical significance using Excel software. One-tailed unpaired t-test with 95% confidence interval was considered statistical significant if $P < 0.05$ (*), $P < 0.01$ (**) and $P < 0.001$ (***).

2.7. Encapsulation and in vitro release of diclofenac

Diclofenac at a concentration of 0.1% (m/v) was added on top of the ChO (0.6 mg/mL) solution prior the addition of xanthan solution (H_2O). These structures could interact for 24 h and dried in an oven at 37 ℃ for 2 h for facili tating the handling of the samples. The dried samples were transferred to a container with 10 mL of PBS, where the release studies were conducted using a Pion μDiss Profiler (Pion, USA) to measure the released drug every minute at wavelength of 280 nm for 2 h. As controls, X-ChO fibers were produced without drugs encapsulated. These studies were conducted in triplicate for each sample. The mechanism of release was investigated using Korsmeyer–Peppas model:

$$(1)\ M_t/M_\infty = Kt^n$$

where M_t/M_∞ is fraction of drug released at time t, K is the rate constant and n is the release exponent. If $n \leq 0.45$, the release mechanism follows a Fickian diffusion and

for $0.45 < n < 0.89$ the drug release follow a non-Fickian diffusion (anomalous transport) [22].

3. Results and discussion

It is know that xanthan assumes an ordered state at specific temperatures and salt concentrations [8,9,23–25]. Optical rotation measurements ($[\alpha]_{436}$) conducted on xanthan solutions at different NaCl concentrations (0–100 mM), confirmed that xanthan dissolved in water at 25 ℃ assumed the non-ordered conformation, while in NaCl 15 mM it appeared in the ordered state (Fig. 2a)[26,27].

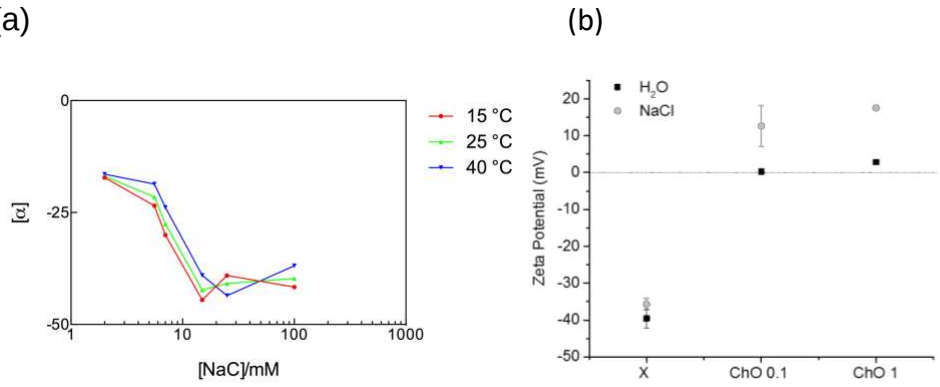

Fig. 2. (a) Variation of the specific optical rotation ($[\alpha]_{436}$) of xanthan gum solutions with NaCl concentration at varying temperatures (as shown in label). Zeta potential (b) of the xanthan (X) and chitosan oligomers (ChO) solutions at concentrations of 0.1 and 1 mg/mL prepared in H_2O and NaCl 15 mM. Presented results are average of at least three independent experiments [N = 3] and are presented as mean ± standard deviation.

Temperatures ranging from 15 to 40 ℃ were observed to do no t affect significantly the optical rotation of xanthan solution as also evinced on Fig. 2a. Fig. 2b shows the zeta potential (ζ) of xanthan and ChO solutions prepared with and without NaCl. The zeta potential of xanthan solution was found to be of −40 ± 3 mV and of −36 ± 2 mV when dissolved in H_2O and NaCl 15 mM, respectively. Positive zeta potential was observed for all the ChO solutions tested, due to the positive charged amino groups of ChO (Fig. 2b). Additionally, the zeta potential was observed to be closed to the isoelectric point for the solutions prepared in H_2O. The deprotonation of the amine groups was shown to be stronger in diluted media and consequently the proximity with isoelectric point is notorious for diluted systems [28]. The increase in concentration of

ChO solutions (from 0.1 to 1 mg/mL) was observed to slightly increase the zeta potential with and without NaCl, as reported elsewhere [28,29]. The presence of salt in solution was also observed to increase the zeta potential of ChO solutions (Fig. 2b). At concentration of 0.1 mg/mL, the zeta potential increased from +0.2 ± 0.01 (H_2O) to +13 ± 6 mV (15 mM NaCl) and at concentration of 1 mg/mL the zeta potential increased from +3 ± 0.1 to +18 ± 0.2 mV. Zeta potential (ζ) measurements confirmed that both components xanthan and chitosan oligomers have opposite charge and hence, they are able to co-assemble by electrostatic interactions. These type of interactions have been shown essential to drive the self-assembly of interfacial systems [2,5,30,31].

By mixing the aqueous solutions of xanthan and ChO an interfacial assembly was observed to spontaneously develop at the interface of both solutions (Fig. 3a,b). The development of sacs-like structures (Fig. 3a) and thin films (Fig. 3b) was observed to depend on the order of mixing (xanthan solution added on top of ChO solutions or vice versa). When the small molecular weight ChO solution was placed on top of the more viscous X solution, a homogeneous thin film, containing fibrilar structures, was observed to form at the interface of both components, covering the whole area of the well, due to the limited diffusion of the small ChO trough the more viscous X solution. On the other hand, placing the dense X solution on top of the less viscous ChO, allows better diffusion of xanthan over ChO solution originating renewal of the liquid-liquid at the interface and thus the formation of a sac like structures.

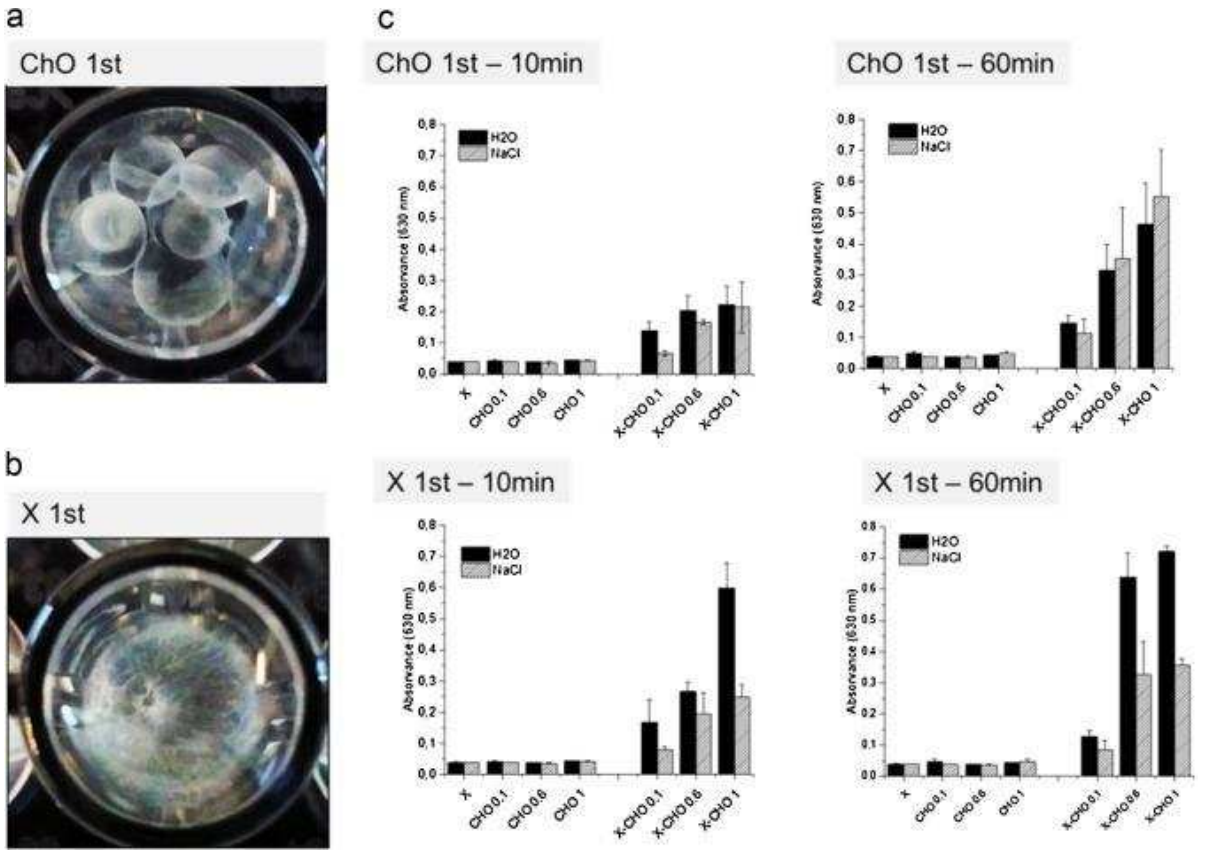

Fig. 3. Digital images of self-assembled X-ChO structures formed on wells using different setup: (a) X solution added on top of ChO solution (ChO 1st); (b) ChO solution added on top of X solution (X1st). (c) Turbidity profiles of X (0.6 mg/mL) and ChO at concentrations of 0.1; 0.6 and 1 mg/mL (control) dissolved in both H_2O and NaCl, and the respective mixtures after 10 and 60 min of interactions. Presented results are average of at least three independent experiments [n= 3] and are presented as mean ± standard deviation.

To investigate the role of NaCl, the concentration of ChO and the incubation time on the electrostatic interactions between xanthan gum and ChO, turbidity studies were performed (Fig. 3c). Individual solutions of X and ChO were used as controls and their absorbance was observed to do not change for the different conditions tested. However, after adding X on top of ChO solution and vice versa, the measured absorbance was observed to increase due to the interactions between components. Overall, the presence of NaCl was observed to decrease the interactions between ChO and X, comparatively to the interactions processed in water. The presence of salts, such as NaCl suppresses the binding of the polyelectrolytes due the screening of electrostatic interactions [32]. Furthermore, as observed previously, the ordered conformation of xanthan when dissolved in 15 mM of NaCl might prevent the access of the small positively charged oligomers to the negative charges of xanthan, thus limiting the interactions comparatively to the solutions prepared in water. Although the

same trend was not observed for the conditions ChO1st -60, the differences between the groups NaCl and H_2O were not statistically significant. The concentration of ChO was observed to play an effect on the X-ChO interactions. Higher ChO concentration interacted strongly with X due to the higher amount of positively charged molecules able to interact with the negatively charged xanthan molecules. This effect was found statistically significant when comparing concentrations of 0.1 and 1 mg/mL. In addition, Fig. 3c demonstrated that the measured absorbance tended to increase with the increase of the time of interactions (from 10 to 60 min). This effect is more pronounced and statistically significant for higher concentrations of ChO such as 1 mg/mL, suggesting that these interactions are time-dependent.

SEM analysis shows the morphology of the self-assembled nano-fibers at different order of mixing, concentrations of ChO, and presence of salt, after 1 and 24 h of interaction (Figs. 4 and 5, respectively). The addition of X on top of ChO solution at 0.1 mg/mL (Fig. 4) originated amorphous surfaces after 1 h. However, when increasing the concentration of ChO, the formation nanofibers were observed at concentrations of 0.6 mg/mL and 1 mg/mL. Similar morphologies were found with solutions prepared in NaCl. The presence of salt was observed to provide more uniform morphology to the nanofibers comparatively to the structures prepared in water due to the suppression of electrostatic binding between the two oppositely charged polyelectrolytes and screening of electrostatic interactions [32].

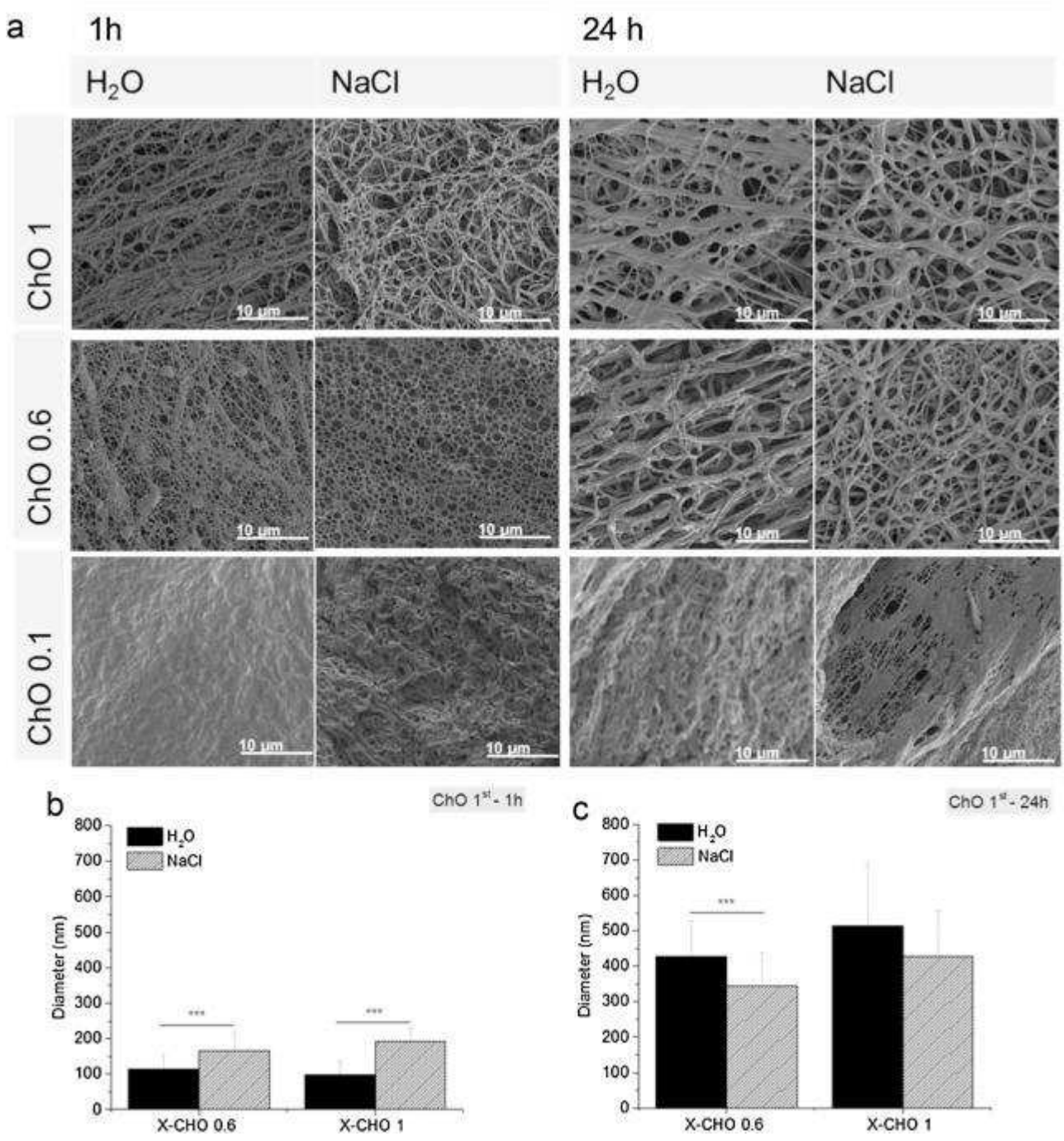

Fig. 4. (a) SEM images of the self-assembled X-ChO nanofibers and the effect of the concentration of ChO, ionic strength (NaCl) and time of incubation (1 and 24 h) on the morphology by adding X on top ChO solution (ChO 1st). Diameter of the self-assembled nanofibers after 1 h (b) and 24 h (c) of interactions between X and ChO. Presented results are average of at least three independent experiments [n = 3] and are presented as mean ± standard deviation.

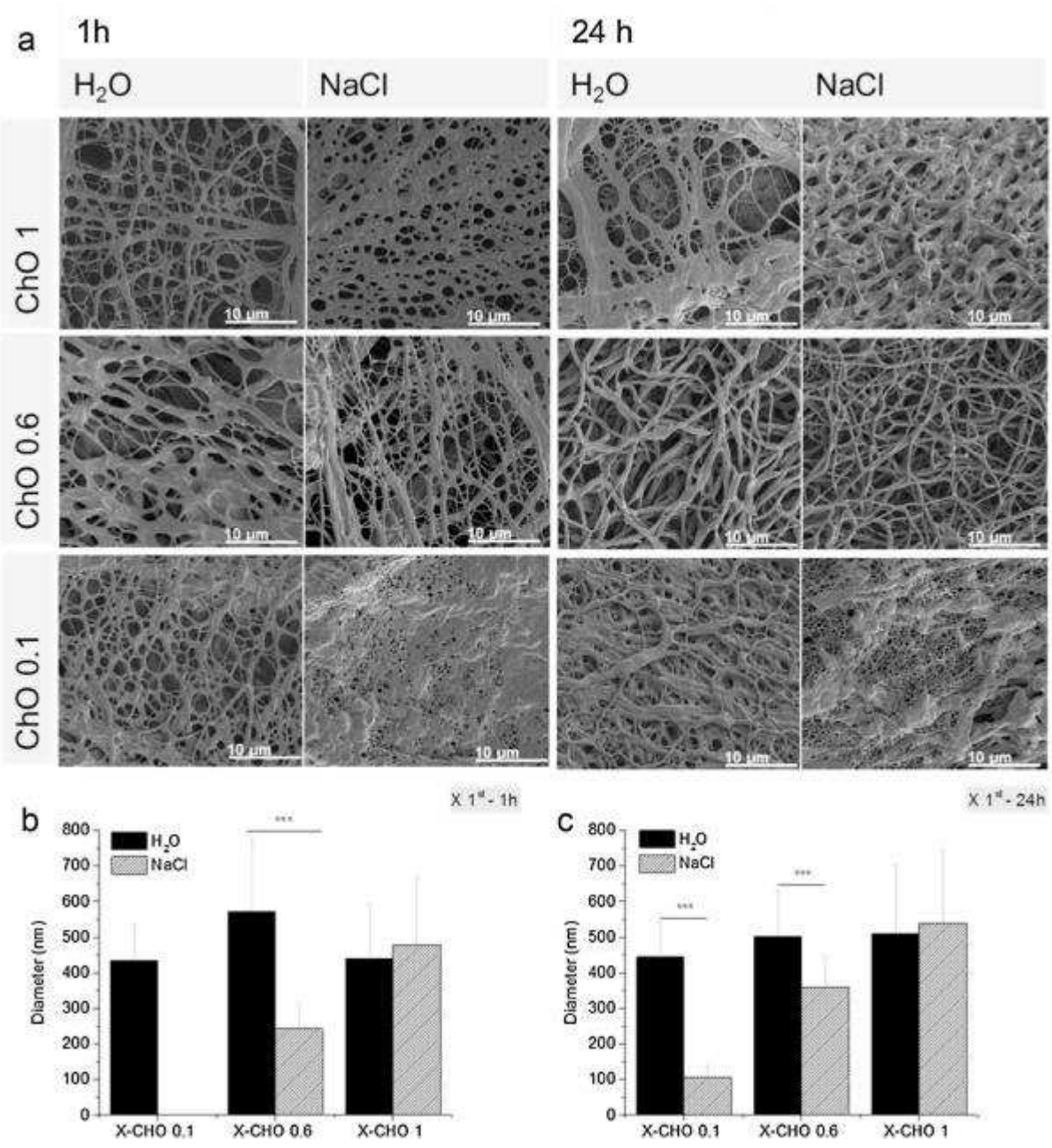

Fig. 5. (a) SEM images of the self-assembled X-ChO nanofibers and the effect of the concentration of ChO, ionic strength (NaCl) and time of incubation (1 and 24 h) on the morphology of the structures fabricated by adding ChO on top X solution (X 1st). Diameter of self-assembled nanofibers after 1 h (b) and 24 h (c) of interactions between X and ChO. Presented results are average of at least three independent experiments [n = 3] and are presented as mean ± standard deviation.

After 24 h of interaction between X and ChO, nanoporous surfaces were observed for concentrations of 0.1 mg/mL and self-assembled nanofibers with increased diameter were observed at concentrations of ChO of 0.6 and 1 mg/mL. The diameters of the

nanofibers were observed to increase from 115 ± 39 (ChO 0.6 mg/mL) and 98 ± 38 nm (ChO 1 mg/mL) to 428.3 ± 100 (ChO 0.6 mg/mL) and 514 ± 170 nm (ChO 1 mg/mL) when using solutions prepared in water. When using xanthan and chitosan oligomers solutions prepared in NaCl, the increase of the nanofibers diameter was observed to duplicate for all concentrations of ChO. Overall, from Fig. 4, it can be seen that the diameter of the nanofibers increased from 1 to 24 h. This time-dependency observed through morphologic analyses is in agreement with turbidity studies discussed previously (Fig. 3c) and is consistent with the self-assembly of molecules bearing opposite charges reported elsewhere [2,30].

Inverting the order of mixing of the components, by adding ChO solution to the X solution, was also investigated (Fig. 5). Adding ChO to xanthan solution led to the formation of nanofibers after 1 h. Nanofibers comprising diameters of 435 ± 88 nm, 572 ± 200 nm and 439 ± 157 nm were produced at concentrations of 0.1, 0.6 and 1 mg/mL respectively. When the solutions were prepared in the presence of NaCl, nanoporous structures were developed at the concentrations of 0.1 mg/mL. Using ChO with concentrations of 0.6 and 1 mg/mL led to the formation of self-assembled nanofibers (Fig. 5). However, in the presence of NaCl, the increase in concentration of the ChO from of 0.6 to 1 mg/mL led to an increase of the nanofiber diameter from 242 ± 75 nm to 478 ± 180 nm, respectively.

After 24 h, the diameter of the nanofibers using the solutions produced in H_2O did not change significantly (Fig. 5c). On the other hand, the presence of salt was shown to reduce the diameter of the nanofibers comparatively to the nanofibers prepared in water. Furthermore, solutions prepared in NaCl, generated nanofibers whose diameters increased upon storage between 1 and 24 h. From 1 to 24 h of interaction between X and ChO, the fibers exhibited an increase in diameter from 243 ± 75 (0.6 mg/mL) and 478 ± 189 (1 mg/mL) to 360 ± 84 (0.6 mg/mL) and 539 ± 202 (1 mg/mL) as observed in Fig. 5. This is attributed to the suppression of the binding of xanthan to chitosan by NaCl [18], which in turn might delay the interactions between both components.

To illustrate a potential application for these nanostructures, the encapsulation and release of Diclofenac, as model drug, was performed in neutral pH. An initial burst release of diclofenac from nanofibers would be expected as it has been demonstrated in previous studies [20,33–35], due to the fastest dissolution of Diclofenac at neutral pH [20]. However, Fig. 6 shows a steady increase in the release of Diclofenac until 60 min from X-ChO nanofibers.

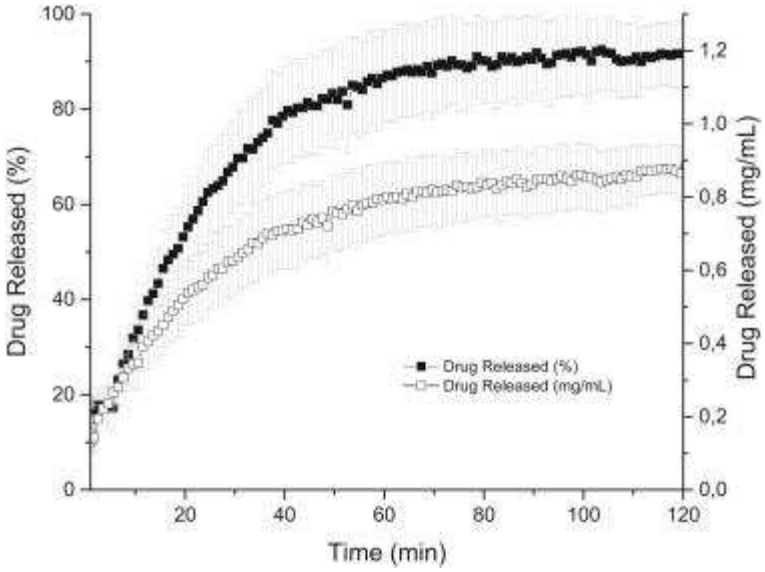

Fig. 6. Release of diclofenac from self-assembled X-ChO nanofibers, in PBS at 37 ℃. Each point represents the average value ± standard error. Presented results are average of at least three independent experiments [n = 3] and are presented as mean ± standard deviation.

From 60 to 90 min a slight increase in the release was observed reaching a plateau at the end of 80 min and releasing about 77% of drug around 120 min. The non-burst release observed suggested the efficient entrapment of the drug within X-ChO self-assembled nanofibers that delayed the dissolution process of diclofenac in PBS [36].

Using Korsmeyer–Peppas model [22], the mechanism of release was determined, through determination of the coefficient “n” estimated from linear regression of the log(Cumulative Release) as a function of log(Time). The “n” determined for this system was 0.6, with the correlation (R^2) of 0.99, suggesting that the release of diclofenac from xanthan-chitosan self-assembled nanofibers follows an anomalous transport kinetics mechanism that can be regarded as an indicator of both phenomena: drug diffusion in the hydrated matrix and polymer relaxation.

4. Conclusions

Self-assembled nanofibers were produced by interfacial interaction of diluted solutions of chitosan oligomers and xanthan gum. The order of mixing of the components was observed to affect the development of the assemblies and average diameter of the nanofibers. Furthermore the morphologic features of the self-assembled nanofibers were shown to be dependent on the concentration of oligomers in mixture and ionic

strength of solutions in addition to the time of assembling. The increase of the concentration of the ChO and the time of interactions was observed to increase the diameter of the nanofibers. The screening of the biopolymer charges due to the presence of salt was observed to delay the interactions between both components over time and thus provide more uniform nanofibers. In addition, the potential to use these self-assembled nanofibers as drug delivery carriers was demonstrated. Diclofenac was successfully released from X-ChO nanofibers without initial burst release at neutral pH, attesting the potential of these structures to be used in drug delivery applications.

Acknowledgements

This work was supported by the European Union funded project “Nano3Bio” (Grant Agreement No. 613931) under FP7.

References

[1] A.C. Mendes, E.T. Baran, R.L. Reis, H.S. Azevedo Self-assembly in nature: using the principles of nature to create complex nanobiomaterials Wiley Interdiscip. Rev. Nanomed. Nanobiotechnol., 5 (2013), pp. 582-612

[2] A.C. Mendes, K.H. Smith, E. Tejeda-Montes, E. Engel, R.L. Reis, H.S. Azevedo, A. Mata

Co-assembled and microfabricated bioactive membranes Adv. Funct. Mater., 23 (2013), pp. 430-438

[3] A.C. Mendes, E.T. Baran, C. Nunes, M.a. Coimbra, H.S. Azevedo, R.L. Reis Palmitoylation of xanthan polysaccharide for self-assembly microcapsule formation and encapsulation of cells in physiological conditions Soft Matter., 7 (2011), p. 9647

[4] A.C. Mendes, E.T. Baran, R.L. Reis, H.S. Azevedo Fabrication of phospholipid-xanthan microcapsules by combining microfluidics with self-assembly Acta Biomater., 9 (2013), pp. 6675-6685

[5] A.C. Mendes, E.T. Baran, P. Lisboa, R.L. Reis, H.S. Azevedo Microfluidic fabrication of self-assembled peptide-polysaccharide microcapsules as 3D environments for cell culture

Biomacromolecules, 13 (2012), pp. 4039-4048

[6] M. Amaike, Y. Senoo, H. Yamamoto Sphere, honeycomb, regularly spaced droplet and fiber structures of polyion complexes of chitosan and gellan Macromol. Rapid Commun., 19 (1998), pp. 287-289

[7] A.C.A. Wan, E.K.F. Yim, I.C. Liao, C. Le Visage, K.W. Leong Encapsulation of biologics in self-assembled fibers as biostructural units for tissue engineering J. Biomed. Mater. Res. A, 71 (2004), pp. 586-595

[8] B. Katzbauer Properties and applications of xanthan gum Polym. Degrad. Stab., 59 (1998), pp. 81-84

[9] F. García-Ochoa, V.E. Santos, J.a. Casas, E. Gómez Xanthan gum: production, recovery, and properties Biotechnol. Adv., 18 (2000), pp. 549-579

[10] A.C. Mendes, E.T. Baran, R.C. Pereira, H.S. Azevedo, R.L. Reis Encapsulation and survival of a chondrocyte cell line within xanthan gum derivative Macromol. Biosci., 12 (2012), pp. 350-359

[11] V. Balan, L. Verestiuc Strategies to improve chitosan hemocompatibility: a review Eur. Polym. J., 53 (2014), pp. 171-188

[12] R. Jayakumar, D. Menon, K. Manzoor, S.V. Nair, H. Tamura Biomedical applications of chitin and chitosan based nanomaterials—a short review Carbohydr. Polym., 82 (2010), pp. 227-232

[13] Y. Luo, Q. Wang Recent development of chitosan-based polyelectrolyte complexes with natural polysaccharides for drug delivery. Int. J. Biol. Macromol., 64 (2014), pp. 353-367

[14] B. Menchicchi, A. Hensel, F.M. Goycoolea Polysaccharides as bacterial antiadhesive agents and “smart” constituents for improved drug delivery systems against Helicobacter pylori infection. Curr. Pharm. Des., 21 (2015), pp. 4888-4906

[15] H. Yin, Y. Du, J. Zhang Low molecular weight and oligomeric chitosans and their bioactivities

Curr. Top. Med. Chem., 9 (2009), pp. 1546-1559

[16] H. Zhang, J. Mi, Y. Huo, X. Huang, J. Xing, A. Yamamoto, Y. Gao Absorption enhancing effects of chitosan oligomers on the intestinal absorption of low molecular weight heparin in rats Int. J. Pharm., 466 (2014), pp. 156-162

[17] S. Argin-Soysal, P. Kofinas, Y.M. Lo Effect of complexation conditions on xanthan-chitosan polyelectrolyte complex gels Food Hydrocoll., 23 (2009), pp. 202-209

[18] C.-H. Chu, T. Sakiyama, T. Fujii, T. Yano Preparation of a polyelectrolyte complex gel and its pH-dependent swelling behaviour. K. Nishinari, E. Doi (Eds.), Food Hydrocoll. Struct. Prop. Funct., Springer US, Boston, MA (1993), pp. 247-250

[19] A.C.A. Wan, M.F.A. Cutiongco, B.C.U. Tai, M.F. Leong, H.F. Lu, E.K.F. Yim Fibers by interfacial polyelectrolyte complexation – processes, materials and applications Mater. Today, 19 (2016), pp. 437-450

[20] X. Shen, D. Yu, L. Zhu, C. Branford-White, K. White, N.P. Chatterton Electrospun diclofenac sodium loaded Eudragit® L 100-55 nanofibers for colon-targeted drug delivery. Int. J. Pharm., 408 (2011), pp. 200-207

[21] E. Shekarforoush, A. Faralli, S. Ndoni, A.C. Mendes, I.S. Chronakis. Electrospinning of xanthan polysaccharide. Macromol. Mater. Eng., 201700067 (2017), p. 1700067

[22] R.W. Korsmeyer, R. Gurny, E. Doelker, P. Buri, N.A. Peppas. Mechanisms of solute release from porous hydrophilic polymers. Int. J. Pharm., 15 (1983), pp. 25-35

[23] M. Milas, M. Rinaudo. Properties of xanthan gum in aqueous solutions: role of the conformational transition. Carbohydr. Res., 158 (1986), pp. 191-204

[24] I. Capron, G. Brigand, G. Muller. About the native and renatured conformation of xanthan exopolysaccharide. Polymer (Guildf), 38 (1997), pp. 5289-5295

[25] Z.H. Mohammed, A. Haque, R.K. Richardson, E.R. Morris. Promotion and inhibition of xanthan “weak-gel” rheology by calcium ions. Carbohydr. Polym., 70 (2007), pp. 38-45

[26] M. Milas, M. Rinaudo. Conformational Investigation on the bacterial poly-saccharide xanthan

Carbohydr. Res., 76 (1979), pp. 189-196

[27] F. Callet, M. Milas, M. Rinaudo. Influence of acetyl and pyruvate contents on rheological properties of xanthan in dilute solution. Int. J. Biol. Macromol., 9 (1987), pp. 291-293

[28] F. Chem Electromigration Behavior of a Mixture of Chitosan Oligomers at Different Concentrations (2006), pp. 10170-10176

[29] R. Obaidat, N. Al-Jbour, K. Al-Sou’d, K. Sweidan, M. Al-Remawi, A. Badwan. Some physico-chemical properties of low molecular weight chitosans and their relationship to conformation in aqueous solution. J. Solution Chem., 39 (2010), pp. 575-588

[30] R.M. Capito, H.S. Azevedo, Y.S. Velichko, A. Mata, S.I. Stupp. Self-assembly of large and small molecules into hierarchically ordered sacs and membranes. Science, 319 (2008), pp. 1812-1816

[31] K.E. Inostroza-Brito, E. Collin, O. Siton-Mendelson, K.H. Smith, A. Monge-Marcet, D.S. Ferreira, R.P. Rodríguez, M. Alonso, J.C. Rodríguez-Cabello, R.L. Reis, F. Sagués, L. Botto, R. Bitton, H.S. Azevedo, A. Mata. Co-assembly, spatiotemporal control and morphogenesis of a hybrid protein–peptide system. Nat. Chem., 7 (2015), pp. 897-904

[32] K. Nishinari, E. Doi (Eds.), Food Hydrocolloids: Structures, Properties, and Functions, Springer US, Boston, MA (1993)

[33] K. Kanawung, K. Panitchanapan, S. Puangmalee, W. Utok, N. Kreua-ongarjnukool, R. Rangkupan, C. Meechaisue, P. Supaphol. Preparation and characterization of polycaprolactone/diclofenac sodium and poly(vinyl alcohol)/tetracycline hydrochloride fiber mats and their release of the model drugs Polym. J., 39 (2007), pp. 369-378

[34] L. Tammaro, G. Russo, V. Vittoria. Encapsulation of diclofenac molecules into poly(e-caprolactone) electrospun fibers for delivery protection. J. Nanomater., 2009 (2009), pp. 1-8

[35] A.C. Mendes, C. Gorzelanny, N. Halter, S.W. Schneider, I.S. Chronakis. Hybrid electrospun chitosan-phospholipids nanofibers for transdermal drug delivery. Int. J. Pharm., 510 (2016), pp. 48-56

[36] X. Li, Z. Zhang, J. Li, S. Sun, Y. Weng, H. Chen Diclofenac/biodegradable polymer micelles for ocular applications Nanoscale, 4 (2012), p. 4667

E. Shekarforoush, A. Faralli, S. Ndoni, A.C. Mendes, I.S. Chronakis**Electrospinning of xanthan polysaccharide**

Macromol. Mater. Eng., 201700067 (2017), p. 1700067

R.W. Korsmeyer, R. Gurny, E. Doelker, P. Buri, N.A. Peppas**Mechanisms of solute release from porous hydrophilic polymers**

Int. J. Pharm., 15 (1983), pp. 25-35

ArticlePDF (2MB)

M. Milas, M. Rinaudo**Properties of xanthan gum in aqueous solutions: role of the conformational transition**

Carbohydr. Res., 158 (1986), pp. 191-204

ArticlePDF (2MB)

I. Capron, G. Brigand, G. Muller**About the native and renatured conformation of xanthan exopolysaccharide**

Polymer (Guildf), 38 (1997), pp. 5289-5295

ArticlePDF (674KB)

Z.H. Mohammed, A. Haque, R.K. Richardson, E.R. Morris**Promotion and inhibition of xanthan “weak-gel” rheology by calcium ions**

Carbohydr. Polym., 70 (2007), pp. 38-45

ArticlePDF (300KB)

M. Milas, M. Rinaudo**Conformational Investigation on the bacterial poly-saccharide xanthan**

Carbohydr. Res., 76 (1979), pp. 189-196

ArticlePDF (524KB)

F. Callet, M. Milas, M. Rinaudo**Influence of acetyl and pyruvate contents on rheological properties of xanthan in dilute solution**

Int. J. Biol. Macromol., 9 (1987), pp. 291-293

ArticlePDF (321KB)

F. Chem**Electromigration Behavior of a Mixture of Chitosan Oligomers at Different Concentrations**

(2006), pp. 10170-10176

R. Obaidat, N. Al-Jbour, K. Al-Sou'd, K. Sweidan, M. Al-Remawi, A. Badwan**Some physico-chemical properties of low molecular weight chitosans and their relationship to conformation in aqueous solution**

J. Solution Chem., 39 (2010), pp. 575-588

R.M. Capito, H.S. Azevedo, Y.S. Velichko, A. Mata, S.I. Stupp**Self-assembly of large and small molecules into hierarchically ordered sacs and membranes**

Science, 319 (2008), pp. 1812-1816

K.E. Inostroza-Brito, E. Collin, O. Siton-Mendelson, K.H. Smith, A. Monge-Marcet, D.S. Ferreira, R.P.Rodríguez, M. Alonso, J.C. Rodríguez-Cabello, R.L. Reis, F. Sagués, L. Botto, R. Bitton, H.S. Azevedo, A. Mata**Co-assembly, spatiotemporal control and morphogenesis of a hybrid protein–peptide system**

Nat. Chem., 7 (2015), pp. 897-904

K. Nishinari, E. Doi (Eds.), Food Hydrocolloids: Structures, Properties, and Functions, Springer US, Boston, MA (1993)

K. Kanawung, K. Panitchanapan, S. Puangmalee, W. Utok, N. Kreua-ongarjnukool, R. Rangkupan, C.Meechaisue, P. Supaphol**Preparation and characterization of polycaprolactone/diclofenac sodium and poly(vinyl alcohol)/tetracycline hydrochloride fiber mats and their release of the model drugs**

Polym. J., 39 (2007), pp. 369-378

L. Tammaro, G. Russo, V. Vittoria**Encapsulation of diclofenac molecules into poly(e-caprolactone) electrospun fibers for delivery protection**

J. Nanomater., 2009 (2009), pp. 1-8

A.C. Mendes, C. Gorzelanny, N. Halter, S.W. Schneider, I.S. Chronakis**Hybrid electrospun chitosan-phospholipids nanofibers for transdermal drug delivery**

Int. J. Pharm., 510 (2016), pp. 48-56

ArticlePDF (2MB)

X. Li, Z. Zhang, J. Li, S. Sun, Y. Weng, H. Chen**Diclofenac/biodegradable polymer micelles for ocular applications**

Nanoscale, 4 (2012), p. 4667